DOI 10.1007/s10527-023-10284-w
Biomedical Engineering, Vol. 57, No. 2, July, 2023, pp. 132–136. Translated from Meditsinskaya Tekhnika, Vol. 57, No. 2, March–April, 2023, pp. 40–43
Original article submitted February 7, 2022

Modeling of Thermal Processes in Prostate Tumors

M. K. Sedankin,[1,2] A. A. Vasil'eva,[3] A. G. Gudkov,[4,*] V. Yu. Leushin,[1] S. V. Chizhikov,[1] M. P. Neimyshev,[4] and E. N. Gorlacheva[5]

Heat exchange processes in prostate glands containing malignant tumors were modeled mathematically by numerical solution of the heat and mass transfer equation for biological tissues. The test objects were malignant prostate tumors with different specific heat release levels; two versions were modeled: without heating and with heating to 45°C. Data were obtained confirming that microwave radiothermometry can be used in the 3800 MHz band for the diagnosis and treatment monitoring of prostate diseases by a variety of hyperthermia-based methods.

Introduction

The diagnosis of oncological diseases is currently associated mainly with the use of traditional structure-based diagnostic methods (ultrasound, MRI, CT, etc.), as well as laboratory methods for confirmation of diagnoses. These methods have a number of limitations, and laboratory tests are not always sufficient for diagnosis. In addition, a common feature of various methods for the diagnosis and treatment of oncological diseases is that they are not universal, i.e., they are effective for some types of tumors and are ineffective or completely unsuitable for other types. Thus, the entire set of available methods should be used in detecting and treating oncological diseases in order to increase treatment efficacy. Despite the importance of the medical imaging methods employed, there are needs not only to increase their effectiveness, but also to develop new methods for the early diagnosis of diseases without additional dose loading of patients. Heat emission of tumors depends on the rate of tumor growth. Aggressive tumors, which represent the greatest danger, have metabolic rates which are much higher than those of intact tissues. As a result, tumor tissue has a higher local temperature, such that thermometric methods can be effective in cancer diagnosis and the monitoring of cancer treatment. Local increases in prostate temperature can also be due to inflammatory processes contributing to the development of prostate cancer. The only way to measure temperatures inside the body in healthcare organizations without trauma or use of routine radiological methods is by using microwave radiothermometry (MR), which provides noninvasive measurement of tissue temperature at depths of up to 5–7 cm [1].

One promising area for the use of MR is in the diagnosis of prostate diseases. There are currently several approaches to thermotherapy that can be used to treat prostate cancer or hyperplasia and this is increasingly recognized as an additional method for use after surgery, chemotherapy, and radiation therapy. Hyperthermia consists of exposing biological tissues to high temperatures [2]. Depending on the temperature regime, three types of hyperthermia are discriminated: adjuvant (38–41°C), true (43–46°C), and ablative (50–100°C) hyperthermia. Adjuvant hyperthermia is used along with radiation therapy and chemotherapy to improve treatment outcomes and reduce side effects. True hyperthermia produces irreversible damage to cells without necrosis of biological tissues by exposure to energy for 40–60 min, while ablation hyperthermia results in complete necrosis within a few minutes. Ablative hyperthermia technologies are divided according to the form of electromagnetic energy used: radiofrequency ablation [3], microwave ablation [4], high-intensity focused ultrasound (HIFU) [5], and laser ablation [6].

Hyperthermia treatment methods can be divided into three types: local, regional, and general. Local hyperthermia is used for small tumors (3–6 cm) and can be applied with

[1]N. E. Bauman Moscow State Technical University, Moscow.

[2]A. I. Burnazyan Federal Medical Biological Center, Federal Medical Biological Agency of Russia, Moscow.

[3]Department of Biocybernetic Systems and Technologies, MIREA Russian Technical University, Moscow.

[4]Department of Instrumentation Technology, N. E. Bauman Moscow State Technical University, Moscow; E-mail: profgudkov@gmail.com

[5]Department of Industrial Logistics, N. E. Bauman Moscow State Technical University, Moscow.

[*]To whom correspondence should be addressed.

external, intracavity (intraluminal), and interstitial emitters which focus radiation into the tumor volume. Regional hyperthermia is used for large parts of the body and is often used to treat larger tumors located in the greater pelvis and the true pelvis. In the case of deeply located tumors, heating is applied using external applicators which emit non-ionizing radiation. Whole body hyperthermia is used in patients with metastatic disease to sensitize tumors to drugs by exposing the entire body to high temperatures (up to 42°C).

One way or another, these technologies are associated with heating tumor tissue and surrounding tissues, so there is a need to monitor the temperature of the heated area during treatment using thermometric methods. In the case of the prostate, this can be achieved using MR, which is described in more detail in [7–9]. Accurate temperature measurement during hyperthermia can be useful to increase the effectiveness of treatment, as thermometry can potentially provide an objective marker of reaching complete thermal destruction (thermonecrosis) of the tumor, minimizing the likelihood of recurrence. Hypothermia methods are also known, such as cryoablation of tumors [10], based on significant freezing of the tumor (below –40°C) to induce cryonecrosis; however, the present work focuses on hyperthermic methods. Thermometry can be effective for diathermy, where moderate heating to a maximum of 41°C occurs, this being used in physiotherapy [11]. If the microwave antenna is placed on the projection of the prostate, the signal power at its output will be proportional to the radio brightness temperature (RT) of the biological object (BO) beneath the antenna $T_{rad}(r)$, which is related to the physical temperature $T(r)$:

$$T_{rad} = \int_{-\infty}^{\infty} T(r)W(r)dV; \quad (1)$$

$$W(r) = \frac{\frac{\sigma(r)}{2}\left|E(r)\right|^2}{\int_{-\infty}^{\infty} \frac{\sigma(r)}{2}\left|E(r)\right|^2 dV},$$

where $T(r)$ is the thermodynamic temperature of the prostate, $W(r)$ is the radiometric weight function of the antenna, $E(r)$ is the electric field strength of the antenna, and $\sigma(r)$ is the electrical conductivity of biological tissues.

Thus, determination of RT requires information on the radiometric function weight $W(r)$ and the thermodynamic temperature $T(r)$ of the prostate in the presence of a tumor. Calculation of the increase in thermodynamic temperature $\Delta T(r)$ requires numerical solution of the heat and mass transfer equation for the prostate with and without pathology. The aim of the present work was to evaluate the potential of MR in the diagnosis and monitoring of the treatment of prostate diseases based on calculations of RT in the projection of the prostate, which is required for designing a multichannel multifrequency intracavity radiothermograph.

Methods

Detection of prostate diseases requires access to the internal cavities of biological objects, which involves the development of new technical solutions for making intracavity radiothermographs. This was approached here by mathematical modeling of the thermal field of the prostate in the presence of a tumor with and without therapeutic hyperthermia (heating up to 45°C). The scheme for diagnostic examination of the prostate using an intracavity radiothermograph is diagrammed in Fig. 1a. Figure 1b shows

TABLE 1. Thermophysical Parameters of Biological Tissues in the Model BO.

Model parameters	Heat production, k, W/(m·°C)	Blood flow parameters ($\rho_b c_b \omega$), W/(m^3·°C)	Specific heat production, Q_{met}, W/m^3
Fat layer	0.21 [13]	1886.152 [14, 15]	700 [15]
Prostate	0.51 [13]	26,069.42 [14, 15]	700 [15]
Urinary bladder	0.52 [13]	5361.805 [14, 15]	700 [15]
Urethra	0.46 [13]	13,107.77 [14, 15]	700 [15]
Urine	0.56 [13]	0	0
Rectum	0.37 [13]	52,699.72 [14, 15]	700 [15]
Malignant tumor	0.45 [13]	26,069.42 [14, 15]	24,000–72,000

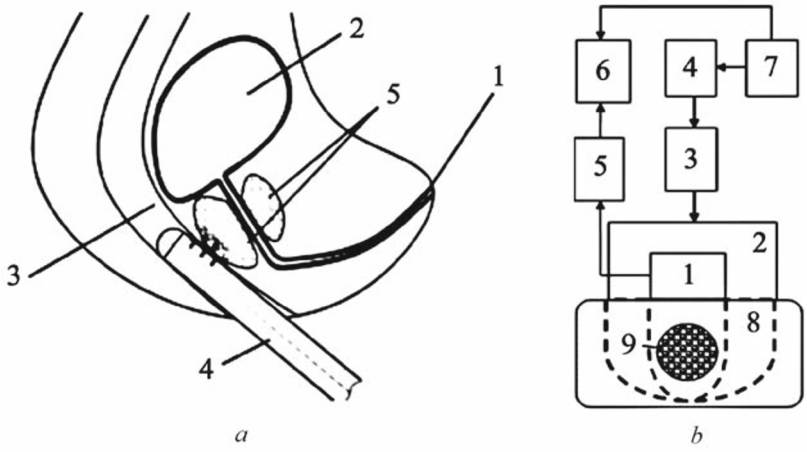

Fig. 1. A simplified scheme for investigating the prostate: 1) urethra; 2) bladder; 3) rectum; 4) intracavity radiothermograph; 5) prostate (a); hyperthermic system with built-in radiothermograph: 1) antenna; 2) hyperthermic emitter; 3) converter (matching device); 4) generator; 5) radiothermograph; 6) data processing module; 7) operator console; 8) BO; 9) malignant tumor (b).

a block diagram of a possible technical implementation of a radiothermograph as part of a hyperthermia system. The thermodynamic temperature of the biological object (BO) is calculated by creating a three-dimensional model of the geometry of the pelvic organs in the presence of a prostate carcinoma (Fig. 2). The geometry of the model, data on the anatomy of the pelvic organs, and other features were analyzed and selected on the basis of reports [4, 10, 12, 13] and the thermophysical parameters of the BO [4, 10, 14, 15] are given in Table 1. The temperature distribution in the BO was calculated by numerical solution of Eq. (2) for a multilayer BO without taking consideration of the antenna design:

$$\nabla \cdot k\nabla T + Q_{met} - \rho_b c_b \omega (T - T_b) = 0, \qquad (2)$$

where T is thermodynamic temperature, ^{o}C; k is the thermal conductivity of the tissue, W/(m·^{o}C); Q_{met} is specific heat release, W/m^3; $\rho_b c_b \omega$ are blood flow parameters, W/(m^3·^{o}C), and T_b is arterial blood temperature, ^{o}C.

The overall dimensions of the model were selected as 250 × 200 × 200 mm; the dimensions of the remaining structures are shown in Fig. 2. The prostate model is a ball with a diameter of 40 mm, while the bladder component has a diameter of 80 mm with a wall thickness of 4 mm. The diameter of the rectum is 50 mm with a wall thickness of 4 mm. The diameter of the urethra was set at 10 mm with a wall thickness of 1.5 mm. Tumor diameter was selected at 20 mm. Given that normal basal temperature is of about 36.5–37.5^{o}C, rectal surface temperature was taken as 37^{o}C, as were temperatures at all external boundaries of the model. Specific heat release was taken as 700 W/m^3 for all biological tissues, i.e., the same as the specific heat release of adipose tissue given in [15]. The blood flow parameters

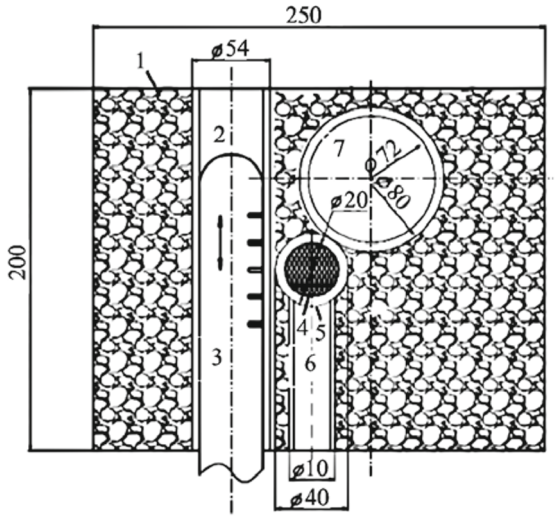

Fig. 2. Model of the pelvic organs (cross section): 1) fat layer; 2) rectum; 3) antenna array; 4) prostate; 5) malignant tumor; 6) urethra; 7) bladder (dimensions are given in millimeters).

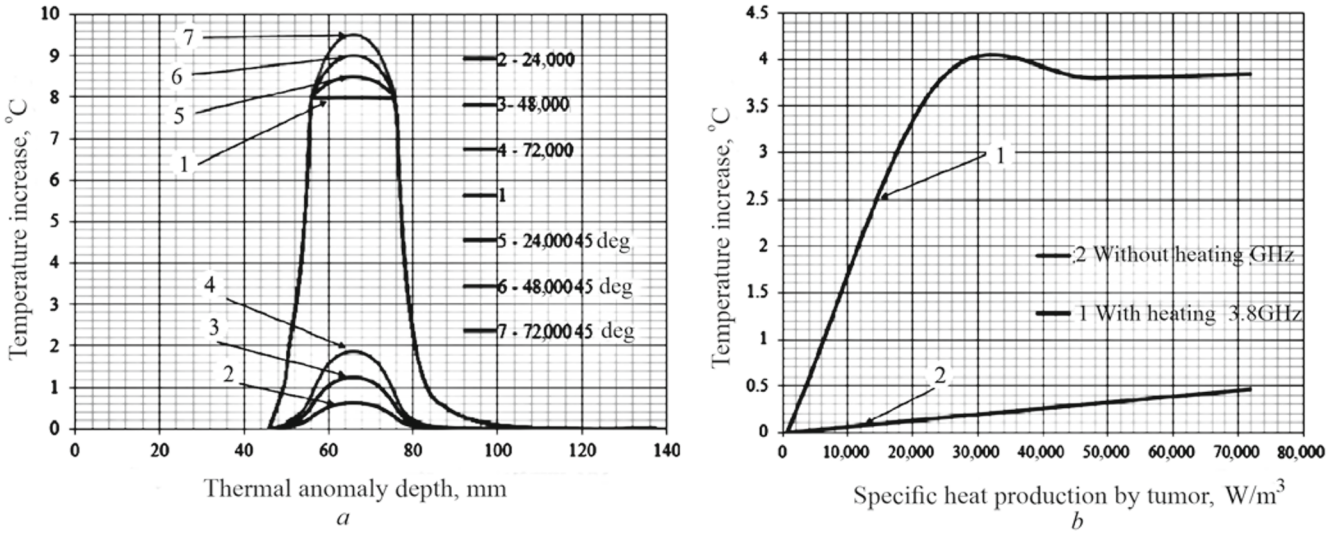

Fig. 3. Temperature distribution in the projection of the prostate without pathology at 45°C (1), with different tumor metabolic rates from 24,000 to 72,000 W/m^3 without heating (2–4) and with heating to 45°C (5–7) (a); increased RT in the 3.8 GHz band in the projection of the thermal anomaly depending on the specific heat release of the tumor on heating to 45°C (1) and without heating (2) (b).

$\rho_b c_b \omega$ for all biological tissues were calculated using data given in [14] as described in [15]. The specific heat release of the tumor was set in the range of 24,000–72,000 W/m^3 by analogy with breast carcinoma [15].

The model of the pelvic organs includes the following assumptions: heat exchange between biological tissues and blood occurs in the capillary bed; heat exchange between large vessels and surrounding tissues is not taken into account; layers of biological tissue are isotropic and homogeneous in terms of thermal characteristics; the thermophysical properties of biological tissues do not depend on temperature; arterial blood temperature T_b = 37°C; convection between layers of the BO is not taken into account as heat exchange occurs only through thermal conduction; the shapes of the model layers are spherical, though the shape of a real BO may differ from a sphere; gas-containing cavities (the rectum and urethra) are filled with air, though in the human body they may contain a mixture of various gases due to life activity; modeling hyperthermic heating of a tumor assumes that the tumor is uniformly heated to 45°C. Furthermore, the thermodynamic temperature distribution was calculated with $T(r)$ and without a tumor $T_0(r)$. The difference (thermal asymmetry) between the resulting temperatures $\Delta T(r)$ was then calculated using Equation (3), which characterizes the effect of the tumor on the temperature distribution.

$$\Delta T(r) = T_0(r) - T(r) . \quad (3)$$

Analogous calculations were carried out with uniform heating of the tumor to a temperature of 45°C, as with heating for therapeutic hyperthermia. The calculation results are shown in Fig. 3a.

Then, by analogy with Eq. (3), the RT $T_{rad}(r)$ was calculated in the 3.8 GHz band over the projection of the prostate tumor using Eq. (1). We used data on the distribution of the electric field (a weighting function that takes account of the contributions of the different layers of the BO to the RT) of an intracavity antenna array built previously in this study and described in [8]. The increase in RT in the projection of the prostate was then calculated using Eq. (4), which is analogous to Eq. (3), without $T_{rad}(r)$ and with a tumor $T_{rad0}(r)$:

$$\Delta T_{rad}(r) = T_{rad0}(r) - T_{rad}(r) . \quad (4)$$

The calculation results are shown in Fig. 3b. Without heating, increases in RT (> 0.3°C) in the presence of a tumor were detectable only at specific heat release of ≥ 48,000 W/m^3. At the same time, heating to 45°C led to significant increases in RT being recorded in the 3.8 GHz band — by up to 4°C.

Conclusions

Heat release and heat transfer processes in the prostate in the presence of tumors were modeled by solving heat

and mass transfer equations. Calculation of the temperature distribution in the prostate containing a malignant tumor, without a tumor, and on exposure to therapeutic hyperthermia (to 45°C) confirmed that MR can be used for the diagnosis of prostate diseases and monitoring their treatment. The data obtained can be used for complex studies using phantoms of malignant neoplasms seeking to improve radiobrightness temperature measurement accuracy using multichannel multifrequency radiothermographs in the depths of a BO, as well as for verifying algorithms and a program for reconstructing the 3D temperature field.

This work was funded by the Russian Science Foundation, agreement No. 19-19-00349-*P* of May 19, 2022 "Creation of method and multichannel multi-frequency microwave radiothermograph based on monolithic integrated circuits for finding the 3D distribution and dynamics of radio brightness temperature within the human body."

REFERENCES

1. Gulyaev, Yu. V. et al., "Instruments for the diagnosis of pathological changes in the human body using microwave radiometr," Nanotekhnol. Razrabot. Primen. XXI Vek, **9**, No. 2, 27–45 (2017).
2. Andreozzi, A. et al., "Modeling heat transfer in tumors: A review of thermal therapies," Ann. Biomed. Eng., **47**, No. 3, 676–693 (2019).
3. Aydin, A. M. et al., "Focal bipolar radiofrequency ablation for localized prostate cancer: Safety and feasibility," Int. J. Urol., **27**, No. 10, 882–889 (2020).
4. Kabiri, A. and Talaee, M. R., "Theoretical investigation of thermal wave model of microwave ablation applied in prostate cancer therapy," Heat Mass Transf., **55**, No. 8, 2199–2208 (2019).
5. Cordeiro, E. R. et al., "High-intensity focused ultrasound (HIFU) for definitive treatment of prostate cancer," BJU Int., **110**, No. 9, 1228–1242 (2012).
6. Natarajan, S. et al., "Focal laser ablation of prostate cancer: Phase I clinical trial," J. Urol., **196**, No. 1, 68–75 (2016).
7. Sedankin, M. K. et al., "Intracavity thermometry in medicine," Biomed. Eng., **55**, No. 3, 224–229 (2021).
8. Sedankin, M. K. et al., "Conformal antenna array for gynecology for medical microwave radiothermograph," in: 2022 International Conference on Actual Problems of Electron Devices Engineering (APEDE), IEEE, **1**, 91–95 (2022).
9. Sedankin, M. K. et al., "Radiometry of the pelvic organs," Biomed. Eng., **53**, 288–292 (2019).
10. Zhang, J. et al., "Numerical simulation for heat transfer in prostate cancer cryosurgery," J. Biomed. Eng., **127**, No. 2, 279–294 (2005).
11. Vrba, D. et al., "Applications of microwaves in medicine and biology," in: Recent Microwave Technologies (2022); https://www.intechopen.com/chapters/82420 (date accessed: January 26, 2023).
12. Kouloulias, V. et al., "Documentation of a new intracavitary applicator for transrectal hyperthermia designed for prostate cancer cases: A phantom study," J. Med. Phys., **43**, 141–145 (2018).
13. El-Gohary, S. H. et al., "Design study on photoacoustic probe to detect prostate cancer using 3D Monte Carlo simulation and finite element method," Biomed. Eng. Lett., **4**, No. 3, 250–257 (2014).
14. Hasgall, P. et al., "IT'IS Database for thermal and electromagnetic parameters of biological tissues (Ver. 4.1), Elsevier, Boston, FL, USA (2022).
15. Said Camilleri, J. et al., "Review of thermal and physiological properties of human breast tissue," Sensors, **22**, No. 10, 3894 (2022).